Journal of Catalysis 256 (2008) 226–236

Contents lists available at ScienceDirect

Journal of Catalysis

www.elsevier.com/locate/jcat

Enantioselective epoxidation of β-methylstyrene catalyzed by immobilized Mn(salen) catalysts in different mesoporous silica supports

Haidong Zhang [a], Yi Meng Wang [b], Lei Zhang [a], Gijsbert Gerritsen [b], Hendrikus C.L. Abbenhuis [b], Rutger A. van Santen [b,*], Can Li [a,*]

[a] State Key Laboratory of Catalysis, Dalian Institute of Chemical Physics, Chinese Academy of Sciences, Dalian 116023, China
[b] Schuit Institute of Catalysis, Eindhoven University of Technology, 5600 MB Eindhoven, The Netherlands

ARTICLE INFO

Article history:
Received 21 January 2008
Revised 16 March 2008
Accepted 17 March 2008
Available online 29 April 2008

Keywords:
Chiral catalysis
Mn(salen)
Asymmetric epoxidation
Motion restriction
Confinement effect
Mesoporous
Immobilization

ABSTRACT

Mesoporous silica-supported chiral Mn(salen) catalysts were prepared and evaluated in the heterogeneous asymmetric epoxidation of β-methylstyrene with NaClO as an oxidant. Homogeneous and immobilized Mn(salen) catalysts exhibit similar *cis*/*trans* ratios and ee values when *trans*-substrate is used but different *cis*/*trans* ratios and ee values when *cis*-substrate is used. The production of *trans*-epoxides is favored in the heterogeneous asymmetric epoxidation of *cis*-β-methylstyrene, whereas the production of *cis*-epoxides is favored in homogeneous reaction. In addition, the *cis*/*trans* ratio and ee value of *trans*-epoxides produced from *cis*-β-methylstyrene change sequentially with changes in support materials, but the ee value of *cis*-epoxides does not. The textural properties of immobilized Mn(salen) catalysts can be sequentially adjusted by changing pore dimension and channel length, after which the motion restriction and confinement effect in nanochannels of immobilized Mn(salen) catalysts can be adjusted sequentially. Our results reflect that the collapse step of *trans*-intermediates is considerably affected by the confinement effect, whereas the rotation step of *cis*-intermediates is greatly influenced by motion restriction. The motion restriction in nanochannels increases the likelihood of rotation for the C–C single bond of *cis*-intermediates and favors the production of *trans*-epoxides.

1. Introduction

Chiral Mn(salen) complex-catalyzed enantioselective epoxidation reactions of unfunctionalized olefins are of great importance in asymmetric catalysis [1–3]. In homogeneous systems, recycling of catalysts and separation of products and catalysts are usually costly multistep processes. Because of the inherent advantages of heterogeneity, including easy separation and recycling, heterogeneous asymmetric epoxidation catalyzed by immobilized Mn(salen) catalysts is of significant interest [4–9]. However, the nanochannels of the supports may exert an unexpected effect on asymmetric catalytic performance; such an effect due to heterogeneity remains an open issue.

Heterogeneous Mn(salen) catalysts can be immobilized with linkage groups connected to the Mn atoms [10–13] or salen ligands [14–22]. Support is a crucial factor influencing the catalytic behavior of immobilized Mn(salen) catalysts at every level; thus, choosing the proper support is critical to formulating an effective immobilization strategy [8,23–25]. Various materials (e.g., alumina, mesoporous silica materials, polymers, carbon materials, zeolites) can be used as the supports of immobilized Mn(salen) catalysts [6–9,23–25]. Among these supports, the mesoporous silica materials, particularly SBA-15 and MCM-41 materials, have received much attention because of their large surface areas, uniform hexagonally ordered two-dimensional mesoporous channels, high hydrothermal stability, and tunable pore dimension and channel structure, allowing ready diffusion of reactants to the active sites located in the nanopores. More importantly, the nanopores of these mesoporous supports can influence the mechanism of the heterogeneous epoxidation reaction [25,26], resulting in a different product distribution than seen in homogeneous reactions. Piaggio et al. found that in the epoxidation of (*Z*)-stilbene catalyzed by MCM-41-immobilized Mn(salen) catalyst with PhIO as an oxidant, the *cis*/*trans* ratio was much higher for heterogeneous reactions than for homogeneous reactions [27], due to retardation of the rotation of the radical intermediates by the MCM-41 nanopores in heterogeneous reactions. The lifetime of the radical intermediates, which is greatly affected by their diffusion behaviors in the nanopores of supports, is another possible factor influencing the rotation step [28].

The mechanism of nanopore-induced changes in product distribution remains unclear, however. In the present work, we immobilized Mn(salen) catalysts in the nanochannels of different

* Corresponding authors. Faxes: +31 40 2455054, +86 411 84694447.
E-mail addresses: r.a.v.santen@tue.nl (R.A. van Santen), canli@dicp.ac.cn (C. Li).
URLs: http://www.catalysis.nl (R.A. van Santen), http://www.canli.dicp.ac.cn (C. Li).

0021-9517/$ – see front matter
doi:10.1016/j.jcat.2008.03.013

mesoporous silica materials with varying pore dimensions and channel structures. The heterogeneous Mn(salen) catalysts were immobilized in two different strategies, in which linkage groups were connected to either Mn atoms or salen ligands. All immobilized Mn(salen) catalysts were evaluated in the epoxidation of β-methylstyrene with NaClO as the oxidant to study the effect of different nanochannels on the reaction. We found that a narrow pore and a long channel increase the selectivity to *trans*-epoxides in the epoxidation of *cis*-β-methylstyrene, consistent with a decreased mobility of reaction intermediates. The motion restriction in narrow pores and long channels can increase the likelihood of C–C single-bond rotation of *cis*-intermediate and favors the production of *trans*-epoxides. In addition, the ee value for *trans*-epoxides varies with changing support, but that for *cis*-epoxides does not, indicating a considerable confinement effect of nanopores on the collapse process for *trans*-intermediates but a negligible effect for *cis*-intermediates.

2. Experimental

Tetraethyl orthosilicate (TEOS, ABCR, low metal impurities, tetraethoxysilane 99+%), EO_{20}–PO_{70}–EO_{20} (Pluronic P123, Aldrich), ammonia (25 wt%, Acros), NH_4F (Acros), trimethyl benzene (TMB, Merck), *n*-decane (Merck), 3-aminopropyl-triethoxysilane (APTES) (ABCR), (R,R)-(-)*N*,*N*′-bis(3,5-di-*tert*-butylsalicylidene)-1,2-cyclohexanediaminomangenese(III) chloride (Jacobsen catalyst, Acros, 98%), dichloromethane (CH_2Cl_2, Acros), 3-tert-butyl-2-hydroxybenzaldehyde (Aldrich, 96%), 3,5-di-*tert*-butyl-2-hydroxybenzaldehyde (Aldrich, 99%), (1R,2R)-(-)-1,2-diaminocyclohexane (Aldrich, 98%), paraformaldehyde (Aldrich), diethyl ether (Et_2O, Acros), $NaHCO_3$ (Merck), Na_2SO_4 (Merck), KOH (Merck), $MgSO_4$ (Acros) concentrated hydrochloric acid (HCl, Acros, 37%), Mn(OAc)2·$4H_2O$ (Acros), LiCl (Acros), (1S,2S)-*trans*-β-methylstyrene oxide (Aldrich, 98%), (1R,2R)-*trans*-β-methylstyrene oxide (Aldrich, 97%), *trans*-β-methylstyrene (Aldrich, 99%), *cis*-β-methylstyrene (TCI, stabilized with TBC, > 98% GC), 4-phenylpyridine *N*-oxide (PPNO, Acros), and *m*-chloroperoxybenzoic acid (*m*-CPBA, Acros) were obtained from commercial sources and used as received. Toluene (Acros) used in the synthesis of 3-aminopropyl-siloxy group modified supports was dried before use.

The content of Mn in the immobilized catalysts was determined by inductively coupled plasma-atomic emission spectrometry (ICP-AES) on an Varian Vista spectrometer. The ^{1}H NMR spectra were recorded on a Bruker Mercury 400 instrument (400 MHz, $CDCl_3$, 25 °C). N_2 adsorption–desorption analysis was done at 77 K on a Micromeritics TriStar 3000 instrument. The small-angle X-ray diffraction (SXRD) patterns were collected on a Rigaku D/max-2500/PC X-ray diffractometer with Cu$K\alpha$ radiation. FTIR spectra were recorded on a Perkin–Elmer Spectrum One FTIR spectrometer with a FR-DTGS detector, using the KBr pellet method at a resolution of 4 cm^{-1}. UV–vis DRS spectra were obtained on a Shimadzu 2010 instrument. High-resolution scanning electron microscopy (HRSEM) was done with a FEI QUANTA 200F instrument or a Philips XL30 FEG instrument. Transmission electron microscopy (TEM) was performed using an FEI Tecnai 20 Twin instrument.

2.1. Synthesis of support materials

2.1.1. Synthesis of mesostructured cellular foams

Synthesis of the mesostructured cellular foam (MCF) supports was done as reported previously [29]. First, 16.67 g of P123 was added to 400 ml of an aqueous 1.67 M HCl solution under stirring at room temperature. Once a clear solution was obtained, 0.1875 g of NH_4F and 12.5 g of TMB were successively added. The mixture was stirred at 35 °C for 3 h, after which 35.53 g of TEOS was added. This mixture was refluxed at 35 °C for 20 h and then hydrothermally treated in an autoclave at 100 °C for 48 h. The mixture was then filtered to collect the white solid product, which was washed with copious amounts of water and dried at room temperature. Finally, the white powder was calcined at 540 °C for 4 h to remove the template agent.

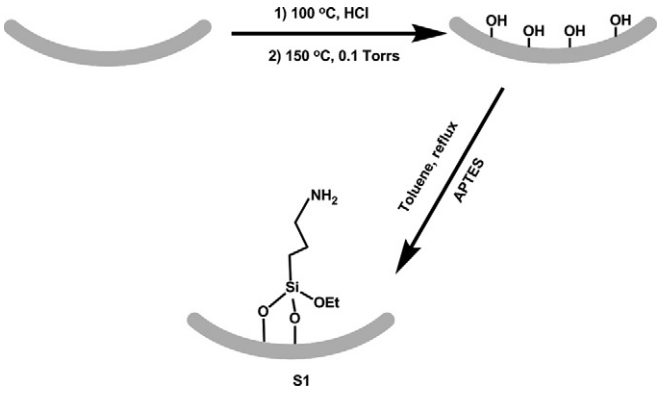

Scheme 1. Preparation of 3-aminopropyl-siloxy group-modified supports.

2.1.2. Synthesis of long-axis SBA-15 support

The synthesis procedure of long-axis SBA-15 (LS) supports was similar to that described by Choi et al. [30]. First, 22.79 g of P123 was added to 700 ml of aqueous HCl solution (0.43 M). The resulting mixture was stirred at room temperature to obtain a clear solution. Then the solution was balanced at 35 °C, followed by the addition of 52.5 ml of TEOS. This mixture was refluxed at 35 °C for 24 h, and then treated in an autoclave at 100 °C for 24 h. The resulting white solid product was then separated by filtration and washed with a mixture of H_2O, ethanol, and HCl, and then dried at room temperature. The dry white powder was then calcined at 550 °C for 4 h to remove the template agent.

2.1.3. Synthesis of short-axis SBA-15 support

To synthesize the short-axis SBA-15 (SS) support, first, 5.04 g of P123 was added to 175 ml of aqueous HCl solution (1.07 M) under stirring at room temperature. When a clear solution was obtained, *n*-decane was added to obtain a mixture with an *n*-decane/P123 molar ratio of 237. The resulting mixture was then stirred overnight. After stirring, the clear separation of a water-rich layer and a decane-rich layer was achieved after at least 8 h. The upper decane-rich layer was carefully removed, and 0.06 g of NH_4F was added to the water-rich layer. The water-rich layer was then stirred at 40 °C for 15 min, followed by the addition of TEOS to achieve a TEOS/P123 molar ratio of 41.4. This mixture was refluxed at 40 °C for 20 h and then hydrothermally treated in an autoclave at 100 °C for 51 h. The mixture was then filtered to collect the white solid product, which was washed with copious amounts of water and dried at 60 °C in vacuum. Finally, the white powder was calcined at 550 °C for 4 h to remove the template agent.

2.2. Synthesis of 3-aminopropyl-siloxy group-modified supports

The preparation of 3-aminopropyl-siloxy group-modified support is demonstrated in Scheme 1. First, 2 g of support was treated by 200 ml of HCl (2 M) at 100 °C for 4 h. The support was then filtered and washed with copious amounts of water until the used filtrate was neutral, and then dried at 40 °C under vacuum overnight. The dried support was dehydrated at 150 °C at 0.1 Torr for 4 h, followed by the addition of 50 ml of dry toluene and 6.9 ml of APTES. The resulting mixture was refluxed at 110 °C under the protection of argon for 18 h, and filtered. The solid support was

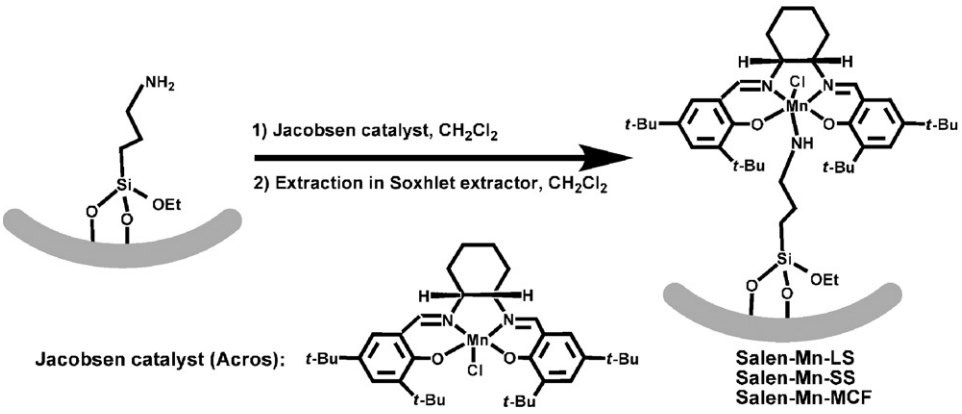

Scheme 2. Preparation of immobilized Mn(salen) catalysts with the linkage groups axially connected to Mn atoms.

washed successively with toluene, acetone, and methanol and then dried at room temperature under vacuum for 4 h.

2.3. Preparation of immobilized Mn(salen) catalysts with the linkage groups axially connected to Mn atoms

The preparation of immobilized Mn(salen) catalysts with the linkage groups axially connected to Mn atoms is schematically illustrated in Scheme 2. First, 2 g of 3-aminopropyl-siloxy group-modified support and 0.1 g of (R,R)-(-)*N*,*N*′-bis(3,5-di-*tert*-butylsalicylidene)-1,2-cyclohexanediaminomangenese(III) chloride (Jacobsen catalyst, Acros, 98%) were added to 40 ml of CH_2Cl_2 under stirring at 20 °C and keep stirring for 16 h. The resulting light-brown solid products were separated by filtration, washed with CH_2Cl_2, and then extracted by 200 ml of CH_2Cl_2 in a Soxhlet extractor for 24 h. The catalysts were extracted twice to ensure good removal of physically adsorbed Mn(salen) complexes. The extracted solid products were then dried at room temperature in vacuum to remove CH_2Cl_2. These catalysts are designated Salen-Mn-LS, Salen-Mn-SS, and Salen-Mn-MCF.

2.4. Preparation of heterogeneous Jacobsen catalysts via a linkage connected to salen ligand

The chiral Mn(III) salen complex **1** was prepared in the procedures as illustrated in Scheme 3.

2.4.1. Synthesis of 3-tert-butyl-5-(chloromethyl)-2-hydroxybenzaldehyde

To synthesize 3-*tert*-butyl-5-(chloromethyl)-2-hydroxybenzaldehyde (3TB5CMB; C1 in Scheme 3) [31], first, 30.0 g of 3-*tert*-butyl-2-hydroxybenzaldehyde and 11.16 g of paraformaldehyde were added into 112.2 ml of concentrated hydrochloric acid. The resulting mixture was stirred at 25 °C for 48 h and then repeatedly extracted with diethyl ether. The diethyl ether layer was repeatedly washed with saturated aqueous $NaHCO_3$ and brine and then dried over Na_2SO_4. A yellow-white crystalline solid (3TB5CMB) was obtained after the evaporation of the solvent in vacuum. ^{1}H NMR ($CDCl_3$, 400 MHz): δ (ppm) 1.43 (s, 9H), 4.58 (s, 2H), 7.42 (d, 1H), 7.52 (d, 1H), 9.87 (s, 1H), 11.86 (s, 1H). FT-IR (KBr): 2967, 2910, 2862, 1650, 1611, 1436, 1268, 1235, 1209, 1162, 979, 772, 697 cm^{-1}.

2.4.2. Synthesis of immobilized Mn(salen) catalysts with linkage group connected to salen ligand

This synthesis was based on a procedure reported by Allen and Jacobsen [32]. First, 0.2127 g of 3TB5CMB, 0.7030 g of 3,5-di-*tert*-butyl-2-hydroxybenzaldehyde, and 0.2284 g of (1R,2R)-(-)-1,2-diaminocyclohexane were added into 10 ml of CH_2Cl_2 (3TB5CMB: (1R,2R)-(-)-1,2-diaminocyclohexane: 3,5-di-*tert*-butyl-2-hydroxybenzaldehyde = 1:2:3). The resulting mixture was stirred at 25 °C for 48 h. The excess of 3,5-di-*tert*-butyl-2-hydroxybenzaldehyde relative to 3TB5CMB yielded a statistical 6:1 ratio of L**2** to L**1**. Then 2 g of 3-aminopropyl-siloxy group-modified support was added into the mixture with 20 ml of CH_2Cl_2 and stirred for 18 h at 25 °C. The selective capture of L**1** and L**2** was allowed, whereas the soluble L**3** was washed away by the CH_2Cl_2 from the support. After the extraction treatment by CH_2Cl_2 in a Soxhlet extractor for 24 h, C**2** was predominant on the supports. Incorporation of a minor amount of L**1** in the catalysts had no apparent deleterious effect on catalyst reactivity or enantioselectivity [32]. Then the immobilization of Mn^{III} salen complexes was accomplished by refluxing an ethanolic solution of 0.3637 g of $Mn(OAc)2{\cdot}4H_2O$ at 90 °C for 1 h, followed by another 30 min at 90 °C after the addition of 0.09538 g of LiCl. The resulting solid products were then washed with CH_2Cl_2 and CH_3OH to obtain light-brown catalysts, designated Mn-Salen-LS, Mn-Salen-SS, and Mn-Salen-MCF.

2.5. Asymmetric epoxidation reaction tests of cis/trans-β-methylstyrene

Racemic *cis*-β-methylstyrene oxides were prepared by the epoxidation of 1 e.q. of *cis*-βmethylstyrene with 1.1 e.q. of *m*-CPBA in CH_2Cl_2 at 0 °C for 24 h [33]. The NaClO solution was prepared as described by Jacobsen et al. [3]. In a typical run of an epoxidation reaction test, a reaction mixture of 0.118 g of *cis/trans*-β-methylstyrene, 0.0175 g of PPNO, 68 μl of *n*-decane, 5 ml of CH_2Cl_2, catalyst (0.0125 g of Jacobsen catalyst for homogeneous runs or 0.2 g of immobilized Mn(salen) catalyst for heterogeneous runs), and 5.5 ml of 0.55 M NaClO (pH 11.3) [3] was stirred at 20 °C until the conversion of *cis/trans*-β-methylstyrene was stable. The reaction process was monitored by chiral GC. The conversion of *cis/trans*-β-methylstyrene, the chemical selectivities of the epoxides, and the ee values of both the *cis*- and *trans*-epoxides were calculated according the chiral GC analysis results obtained on a Carlo Erba 6000 Vega series 2 instrument equipped with a Lipodex E capillary column (25 m, 0.25 mm inner diameter). An internal standard method was used with *n*-decane as the internal standard in all epoxidation reaction tests and calibration runs. In the calibration runs, (1S,2S)-*trans*-β-methylstyrene oxide, (1R,2R)-*trans*-β-methylstyrene oxide, and racemic *cis*-β-methylstyrene oxides were used to set up the calibration curves. Analysis of the products with an Angilent 5975 GC-MS instrument found that benzaldehyde was the main byproduct.

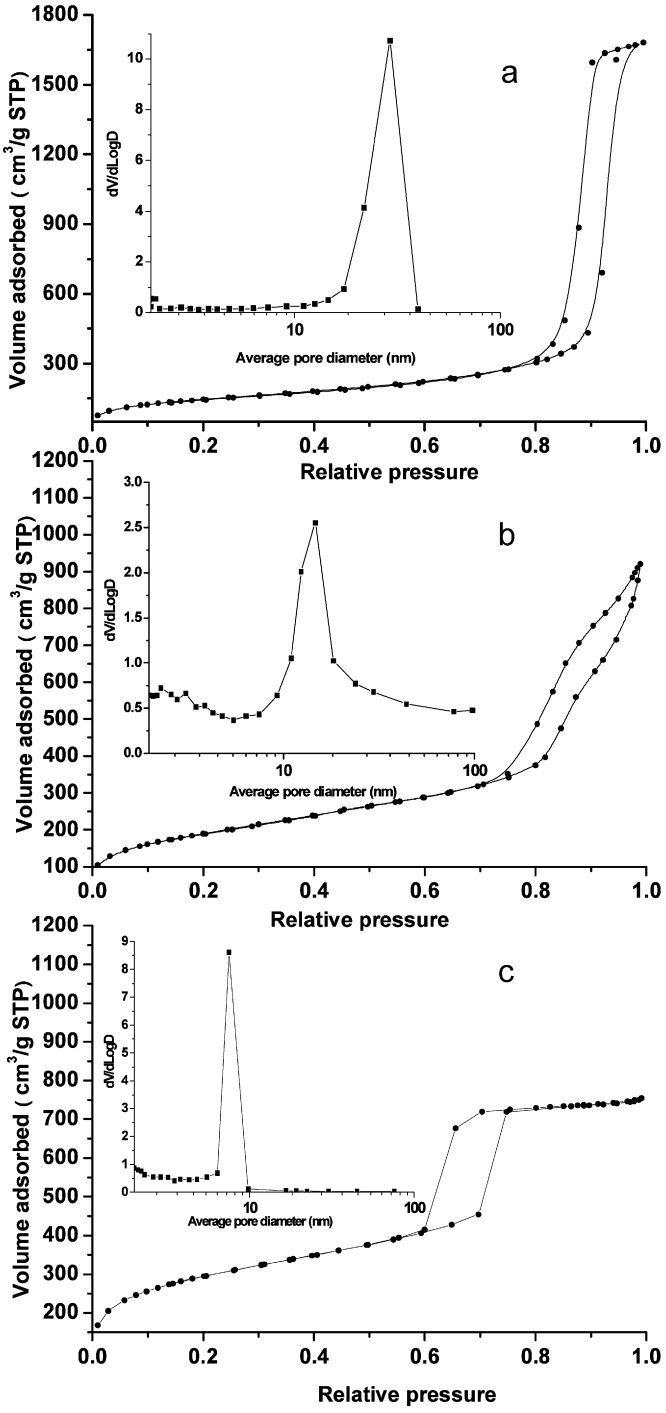

Fig. 1. N_2 adsorption–desorption isotherms of (a) MCF; (b) SS; (c) LS. The insets are pore size distributions by adsorption branch of N_2 adsorption–desorption isotherms.

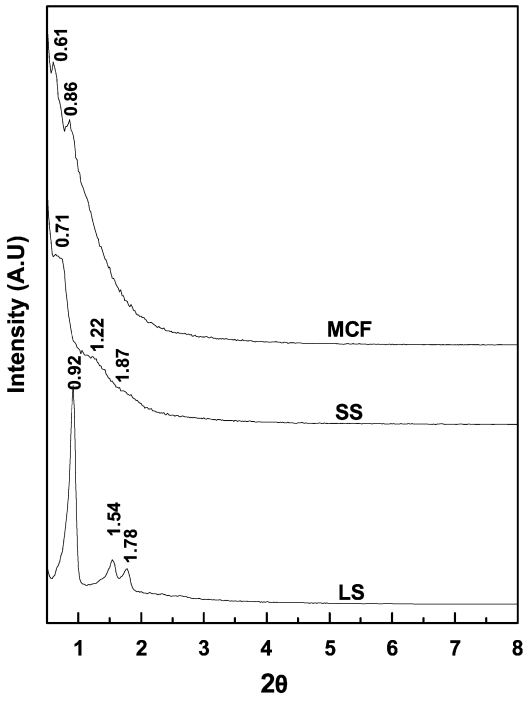

Fig. 2. Small-angle X-ray diffraction patterns of MCF, SS and LS.

3. Results and discussion

3.1. Characterizations of supports and catalysts

3.1.1. Textural and chemical properties of support materials and immobilized catalysts

Fig. 1 shows the N_2 adsorption–desorption isotherms of the MCF, SS, and LS support materials. All of the support materials exhibited representative type IV isotherms [34], with hysteresis loops typical of ordered mesoporous materials with narrow pore size distribution centered around 29.1 nm for MCF, 14.6 nm for SS, and 7.5 nm for LS. The SXRD patterns of the support materials are shown in Fig. 2. In the SXRD pattern of the LS material, three peaks, centered at 0.92°, 1.54°, and 1.78°, were indexed as (100), (110), and (200) diffractions. The SXRD pattern of the SS material exhibited a similar periodic structure. The SXRD patterns of the LS and SS materials confirm a two-dimensional hexagonal symmetry (*p6mm*). Two diffraction peaks at 0.61° and 0.86° were seen in the SXRD pattern of MCF material, suggesting a different periodic structure from that of LS or SS.

According to the HRSEM and TEM images in Fig. 3, the MCF material is composed of large, uniform spherical cells interconnected by uniform windows to create a 3-D pore system. The SS particles exhibit hexagonally ordered channels <300 nm long located along the short axis of these particles. The LS support has hexagonally ordered channels growing along the long axis of the particles with length much greater than 1000 nm. The HRSEM and TEM results of the support materials are in line with the SXRD results shown in Fig. 2. The characteristic pore dimensions and channel structures of these three different support materials remained intact after the heterogenization of Mn(salen) complexes, as shown by the TEM images of the immobilized catalysts in Fig. 4.

Table 1 gives the textural and chemical properties of support materials and immobilized catalysts. The manganese content of the immobilized catalysts was determined by ICP-AES. Both immobilization strategies led to a specific Mn loading. In comparison, pure siliceous support materials without modification of the 3-aminopropyl-siloxy group were first physically mixed with Jacobsen catalyst or a mixture of L**1**, L**2**, and L**3** in CH_2Cl_2, then treated with $Mn(OAc)_2$ and LiCl. All of the resulting mixed solid products were then extracted by CH_2Cl_2 in a Soxhlet extractor. These materials exhibited no activity in the asymmetric epoxidation reaction tests of *cis/trans*-β-methylstyrene according to the GC-MS results. After three uses, no evident change in the textural properties and manganese contents of the LS immobilized catalysts was observed.

The pore diameter and pore volume of the three support materials decreased in the following sequence: MCF > SS > LS. For the immobilized catalysts, with the 3-aminopropyl-siloxy group connected to either the Mn atom or the salen ligand, the pore diameter and pore volume also decrease in the sequence MCF >

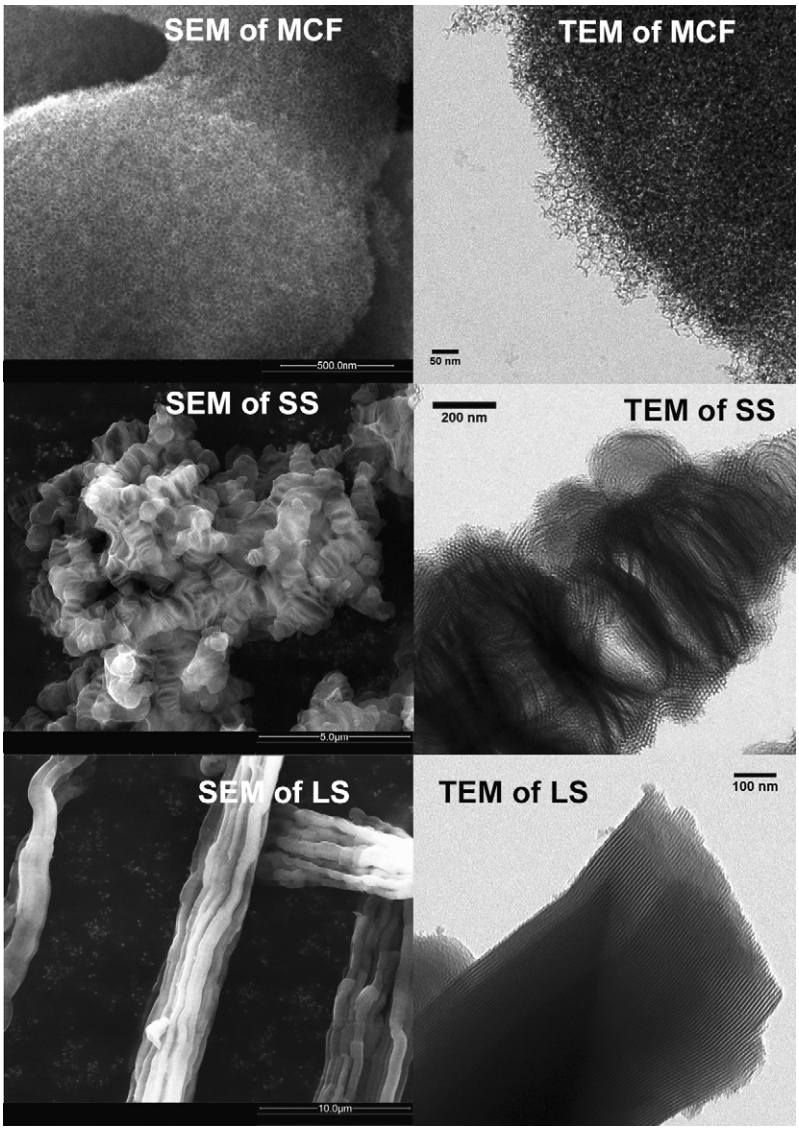

Fig. 3. HRSEM and TEM images of MCF, SS and LS.

SS > LS, as did the channel length of the support materials or the immobilized catalysts (Figs. 3 and 4).

3.1.2. FTIR studies on immobilized catalysts

Fig. 5 shows the FTIR spectra of the support materials and immobilized Mn(salen) catalysts. The bands at 2857, 2922, and 2963 cm^{-1}, which were absent in the spectra of support materials but present in the spectra of all immobilized Mn(salen) catalysts, are attributed to $\nu(CH_2)$ of the propyl arm of the silylating agent, confirming the immobilization of Mn(salen) complex via a tethering linkage group [13,19,22]. In addition, the appearance of the band at 3014 cm^{-1} in the spectra of all immobilized Mn(salen) catalysts can be attributed to the presence of *tert*-butyl groups [22], confirming that the salen ligands with the structure as shown in Schemes 2 and 3 were grafted onto the surface of support materials. Furthermore, new characteristic bands of Mn(salen) centered at 1565, 1550, and 1535 cm^{-1} can be observed in spectra of all immobilized Mn(salen) catalysts, indicating that the chiral Mn(salen) complex was immobilized on the support [13,22]. Each support material exhibited a broad band at around 1635 cm^{-1} due to the O–H bending vibrations of adsorbed water. The C=N groups in the immobilized Mn(salen) catalysts, which participated in coordination with manganese ions, should give a characteristic band overlapped by this O–H bending vibration band [22]. The bands centered at around 1635 cm^{-1} in the spectra of the immobilized Mn(salen) catalysts shifted slightly to lower wavenumbers and increased in intensity, also suggesting immobilization of the Mn(salen) complex on the support materials. Similar results were obtained for all immobilized catalysts, indicating that the different immobilization strategies shown in Schemes 2 and 3 can immobilize the Mn(salen) complex on all three support materials via a tethering linkage group connected to the salen ligand or to the Mn atom.

3.1.3. UV–vis DRS studies on support materials and immobilized catalysts

Fig. 6 shows the UV–vis DRS spectra of the LS immobilized catalyst on LS, and Jacobsen catalyst from Acros. No band can be seen in the spectrum of LS. The spectra of the Jacobsen catalyst and the mechanically mixed LS + Jacobsen catalyst exhibited similar features. The bands at 256 and 296 nm are from the $\pi \rightarrow \pi*$ excitation, and the band at 323 nm is related to the $n \rightarrow \pi*$ excitation of salen ligand. The band at 447 nm is due to the charge-transfer (CT) transition from the salen ligand to the metal [10]. The band at 515 nm is attributed to the d–d transition of Mn(salen) complex [22]. The band at 248 nm was

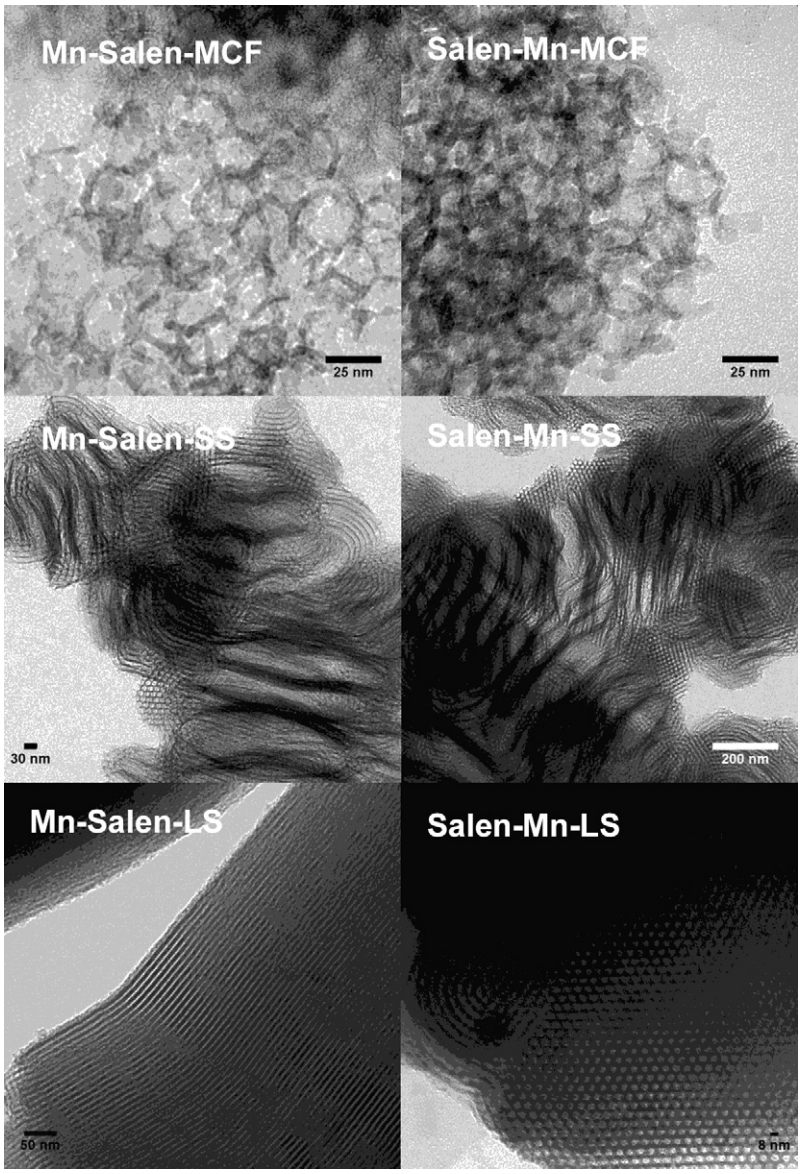

Fig. 4. TEM images of the immobilized catalysts with 3-aminopropyl-siloxy group connected to Mn atom (Salen-Mn-MCF, Salen-Mn-SS and Salen-Mn-LS) or salen ligand (Mn-Salen-MCF, Mn-Salen-SS and Mn-Salen-LS).

Table 1
Textural and chemical properties of support materials and immobilized catalysts

Support materials and immobilized catalysts	Pore diameter (nm)	Specific area (m^2/g)	Pore volume (cm^3/g)	Content of Mn (mg/g)
MCF	29.1	533	2.59	–
SS	14.6	690	1.42	–
LS	7.5	1055	1.11	–
Mn-Salen-MCF	28.2	406	1.76	0.252
Mn-Salen-SS	14.0	573	0.89	0.194
Mn-Salen-LS	6.5	832	0.58	0.236
Salen-Mn-MCF	27.8	389	1.52	0.089
Salen-Mn-SS	13.7	568	0.96	0.079
Salen-Mn-LS	6.2	875	0.62	0.076
Recycled Mn-Salen-LS[a]	6.1	799	0.55	0.240
Recycled Salen-Mn-LS[a]	6.0	811	0.57	0.080

The specific areas were calculated following BET method and the data of pore diameter and pore volume were evaluated by BJH method from adsorption isotherm plots.

[a] Recycled for 2 times; in each recycle, the catalyst was separated by filtration and sequentially washed by distilled water, ethanol, acetonitrile and dichloromethane and then dried at room temperature in vacuum.

detected in the spectrum of S and should be assigned to the C–N group in S1. As shown in Fig. 6a, the spectrum of Salen-Mn-LS shows five bands similar to those for the Jacobsen catalyst and the LS + Jacobsen catalyst. The bands for Salen-Mn-LS centered at 239, 288, 316, 423, and 513 nm exhibited a blue shift compared with those for the Jacobsen catalyst and LS + Jacobsen catalyst, reflecting the interaction between the Mn(salen) complex and the LS support. When the linkage group was connected to salen ligand as shown in Scheme 3, the immobilized salen ligand C2 gave five bands centered at 225, 261, 288, 328 and 416 nm but no d–d transition band at 515 nm. The differences in the spectra of C2 and the Jacobsen catalyst are due to the absence of the Mn atom in the C2 complex. The spectrum of the Mn-Salen-LS catalyst showed bands at 244, 292, 321, and 421 nm and a d–d transition band at 516 nm, confirming the production of immobilized Mn(salen) complex on the support. The minor differences in the spectra of the Mn-Salen-LS and Salen-Mn-LS catalysts reflect the different immobilization strategies for these two catalysts. Similar results were obtained for SS and MCF support materials.

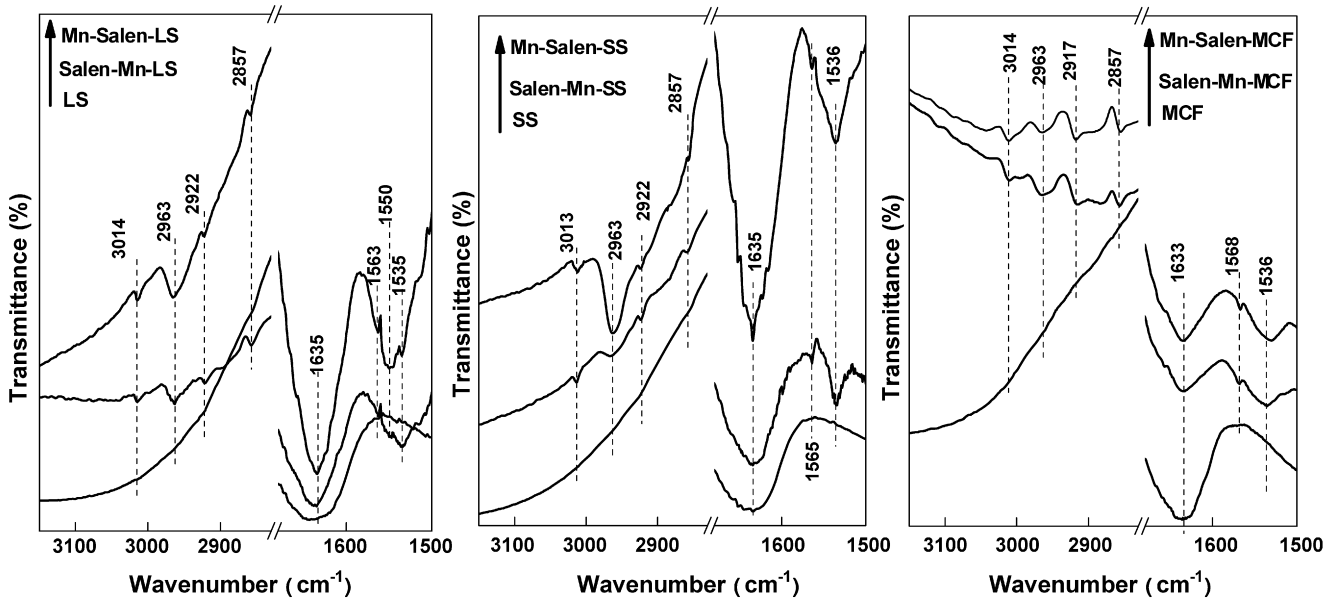

Fig. 5. FT-IR spectra of the immobilized catalysts with 3-aminopropyl-siloxy group connected to Mn atom (Salen-Mn-MCF, Salen-Mn-SS and Salen-Mn-LS) or salen ligand (Mn-Salen-MCF, Mn-Salen-SS and Mn-Salen-LS).

3.2. Enantioselective epoxidation of cis/trans-β-methylstyrene with NaClO as oxygen donor

Table 2 characterizes the catalytic performance of the homogeneous Jacobsen catalyst and the immobilized Mn(salen) catalysts (i.e., Mn-Salen-LS, Mn-Salen-SS and Mn-Salen-MCF) in the asymmetric epoxidation of β-methylstyrene in CH_2Cl_2 with NaClO as an oxidant. The commercial Jacobsen catalyst exhibited almost the same activity, *cis/trans* ratio of epoxides, and enantioselectivity (entries 1 and 5) as were reported by Zhang et al. [35] also with NaClO as an oxidant. After the Mn(salen) complex was immobilized in the nanopores of previous supports, the β-methylstyrene conversion, chemical selectivity, and ee values of the epoxides changed. As shown in Tables 2 and 3, the immobilized Mn(salen) catalysts exhibited significantly lower conversion of substrate and slightly lower TOF values compared with the homogeneous catalyst. This decreased conversion is common in heterogeneous asymmetric catalyzed by epoxidation immobilized Mn(salen) catalysts [4–8,11–22]. In a homogeneous reaction system, the content of homogeneous Mn(salen) catalyst is normally not below 4 mol% [3, 36] against substrate, but was 2 mol% in the present study. The content of immobilized Mn(salen) complex in heterogeneous reactions was significantly lower than that of homogeneous Mn(salen) catalyst in homogeneous reactions, leading to an evident decrease in substrate conversion. When the concentration of Mn(salen) in homogeneous reactions decreased to a level close to that in heterogeneous reactions (about 0.04 mol% against substrate), the conversion of either *cis*-β-methylstyrene or *trans*-β-methylstyrene also decreased dramatically, and the corresponding facial TOF values dropped to levels comparable to those for heterogeneous reactions (1.18×10^{-3} s^{-1} for *cis*-substrate and 2.06×10^{-3} s^{-1} for *trans*-substrate).

The *cis/trans* ratio and the ee values differed between heterogeneous and homogeneous reactions. In the homogeneous reaction, the *cis*-substrate led to more *cis*-epoxides (entry 1, Table 2), in agreement with previous reports [3,35–38]. With *cis*-substrate in the heterogeneous reactions, the production of *cis*-epoxides decreased in following sequence with changing support materials: homo-> MCFs > SS > LS (entries 2, 3 and 4, Table 2). The change in support had no distinct effect on the ee values of the *cis*-epoxides. The corresponding ee value for *trans*-epoxides decreases in the same sequence as found for the production of *cis*-epoxides. When the *trans*-substrate was used in the homogeneous and heterogeneous reactions, only *trans*-epoxides were detected, and the ee value for *trans*-epoxides were constant and low (entries 6, 7, and 8, Table 2). The homogeneous Mn(salen) catalyzed asymmetric epoxidation of *trans*-olefins are always poorly enantioselective according to the side-on approach mechanism [37] and recent results of density functional theory (DFT) and quantummechanics/molecular mechanics (QM/MM) calculations [39]. This is consistent with the poor enantioselectivity for the immobilized Mn(salen) catalyst-catalyzed asymmetric epoxidation of *trans*-β-methylstyrene shown in Tables 2 and 3.

To characterize the effect of different immobilization strategies on product distribution in heterogeneous reactions, Table 3 presents the catalytic data for the axially immobilized Jacobsen catalysts (i.e., Salen-Mn-LS, Salen-Mn-SS, and Salen-Mn-MCF) in the asymmetric epoxidation of β-methylstyrene. The table reports increased *trans*-epoxide production with *cis*-substrate. The *cis*-epoxide production and the ee values for the *trans*-epoxides also decreased in the following sequence: homo-> MCF > SS > LS (entries 2, 3, and 4, Table 3). When *trans*-substrate was used, only *trans*-epoxides were detected, and the ee values changed only slightly (entries 6, 7, and 8, Table 3).

Table 3 shows much lower chemical selectivities for heterogeneous reactions catalyzed by the axially immobilized Mn(salen) catalysts compared with the homogeneous (entries 1 and 5) and heterogeneous reactions catalyzed by the catalysts with linkage groups connected to the salen ligand (entries 2, 3, 4, 6, 7, and 8, Table 2). The recycled Salen-Mn-LS and Mn-Salen-LS catalysts (Table 1, entries 10 and 11) exhibited almost the same activity and ee values but slightly lower chemical selectivity compared with the fresh catalysts. The decomposition reaction of four β-methylstyrene epoxides catalyzed by Salen-Mn-LS (Table 4) exhibited no activity in the long run. It is known that changes in the *cis/trans* ratio and ee values of *trans*-epoxides do not result from the further reaction after the formation of β-methylstyrene epoxides. This suggests that the heterogeneity, resulting from the confinement effect of nanopores and the motion restriction in nanochannels on heterogeneous chiral induction, is the main reason for the varying ee values in our cases [5–7,24,25].

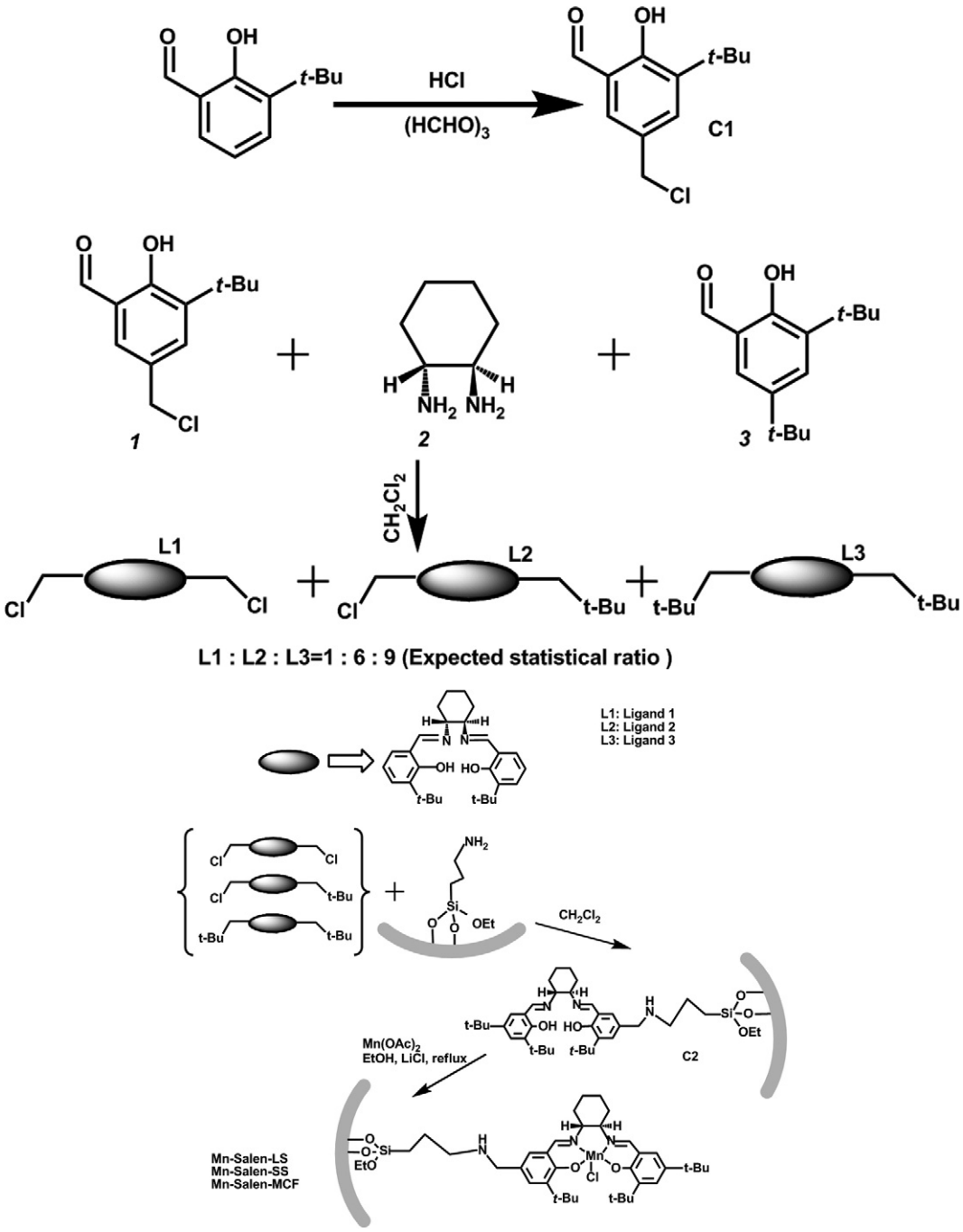

Scheme 3. Preparation of heterogeneous Jacobsen catalysts via a linkage connected to salen ligand.

In the heterogeneous asymmetric epoxidation of *cis*-β-methylstyrene catalyzed by immobilized Mn(salen) catalysts, the radical intermediate with a sp^3 C–C single bond will either collapse to produce *cis*-epoxides (the *cis*-route) or first rotate and then collapse to produce *trans*-epoxides (the *trans*-route), as illustrated in Scheme 4, similar to the reaction in homogeneous asymmetric epoxidation [13,36–42]. At 20 °C, ring closure is the slower process and thus the rate-determining step [36]. The *cis*/*trans* ratio can be reversed by cooling the reaction mixture to −78 °C, which slows the sp^3 C–C single-bond rotation responsible for *cis*/*trans* isomerization sufficiently so that the ring-closure step becomes the faster step [43]. In addition, Chang et al. found that quaternary ammonium salts can induce increased production of *trans*-epoxides in the asymmetric epoxidation catalyzed by Mn(salen) complexes in CH_2Cl_2 with NaClO as an oxygen donor [37]. The ammonium salts extend the lifetime of radical intermediates, thus permitting free rotation of the sp^3 C–C single bond, and then selectively collapse to *trans*-epoxides. According to the reaction results given in Tables 2 and 3, the nanopore wall may play the same role in heterogeneous reactions as ammonium salts do in the homogeneous reaction, resulting in increased *trans*-epoxide production in heterogeneous reactions. Due to the different pore sizes and channel lengths of these three support materials, the motion restriction in the nanochannels of these materials changes in the sequence homo-< MCF < SS < LS, and the production of *trans*-epoxides with *cis*-substrate increases in the same sequence.

The optimal pore size of the support is crucial to achieving enhanced enantioselectivity in nanopores [24,25]. In the asym-

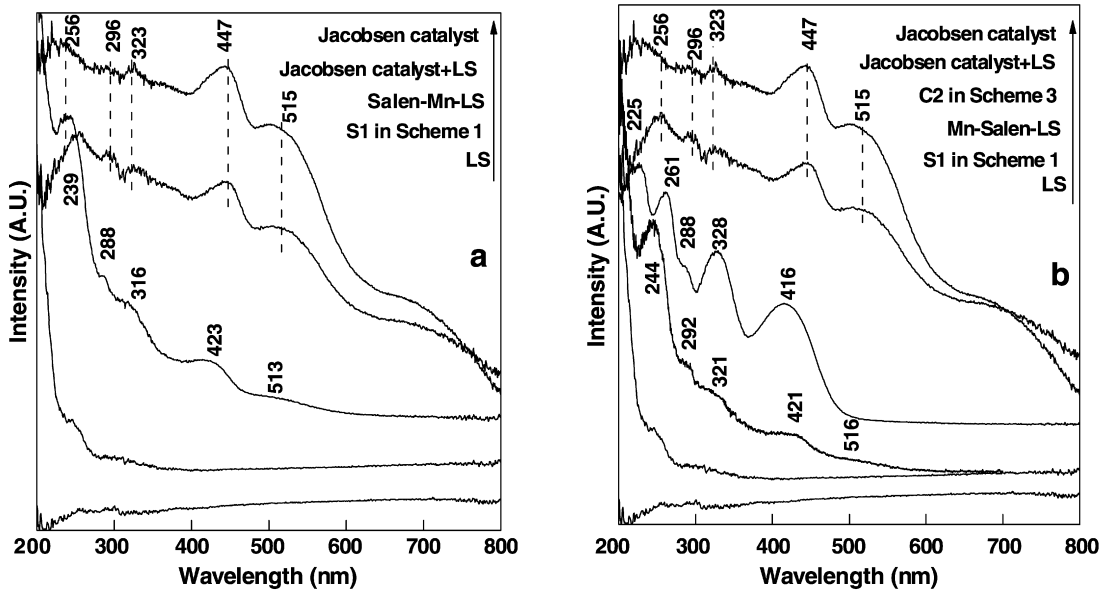

Fig. 6. UV–vis DRS spectra of LS support material, Jacobsen catalyst, mechanically mixed Jacobsen catalyst (Jacobsen catalyst + LS) and (a) Salen-Mn-LS and S1 and (b) Mn-Salen-LS, C2 and S1.

Table 2
Asymmetric epoxidation of β-methylstyrene catalyzed by homogeneous Jacobsen catalyst and immobilized Mn(salen) catalysts (Mn-Salen-LS, Mn-Salen-SS and Mn-Salen-MCF)

Entry	Substrate	Catalyst	t (h)	Conv. (%)	Epoxides sel. (%)			ee (%)		Epoxides config.		Facial TOF ($\times 10^{-3}$ s^{-1})[d]
					Total[a]	*trans*-[b]	*cis*-[b]	*trans*-	*cis*-	*trans*-	*cis*-	
1	*cis*-	Homo-[c]	6	99.5	79.8	15.9	84.1	70.0	83.4	1S,2S	1R,2S	1.84
2		Mn-Salen-MCF	48	22.2	75.0	22.8	77.2	42.8	78.5	1S,2S	1R,2S	1.15
3		Mn-Salen-SS	48	17.8	77.1	43.1	56.9	24.5	78.3	1S,2S	1R,2S	1.08
4		Mn-Salen-LS	24	19.7	68.2	56.0	44.0	6.2	80.5	1S,2S	1R,2S	1.21
5	*trans*-	Homo-[c]	6	100	100	100	n.d.	14.9	–	1R,2R	–	2.31
6		Mn-Salen-MCF	48	66.3	97.4	100	n.d.	11.3	–	1R,2R	–	1.98
7		Mn-Salen-SS	48	31.9	79.6	100	n.d.	10.2	–	1R,2R	–	1.74
8		Mn-Salen-LS	24	29.5	61.6	100	n.d.	7.6	–	1R,2R	–	1.62

Reaction temperature is 20 °C. The blank runs with the mixtures of *cis*/*trans*-methylstyrene, all supports, dichloromethane, *n*-decane and 0.55 M NaClO exhibit that the physical adsorption of *cis*/*trans*-methylstyrene by SBA-15 is negligible.
[a] The molecular proportion of all epoxides in the products.
[b] The molecular proportion of *cis*- or *trans*-epoxide in the summary of all epoxides.
[c] Jacobsen catalyst from Acros.
[d] Facial turnover frequency (TOF) is calculated by the expression [product]/[catalyst] × time (s^{-1}) and according to the reaction data at 6 h; n.d., not detected.

Table 3
Asymmetric epoxidation of β-methylstyrene catalyzed by homogeneous Jacobsen catalyst and axially immobilized Mn(salen) catalysts (Salen-Mn-LS, Salen-Mn-SS and Salen-Mn-MCF)

Entry	Substrate	Catalyst	t (h)	Conv. (%)	Epoxides sel. (%)			ee (%)		Epoxides config.		Facial TOF ($\times 10^{-3}$ s^{-1})[d]
					Total[a]	*trans*-[b]	*cis*-[b]	*trans*-	*cis*-	*trans*-	*cis*-	
1	*cis*-	Homo-[c]	6	99.5	79.8	15.9	84.1	70.0	83.4	1S,2S	1R,2S	1.84
2		Salen-Mn-MCF	48	24.8	39.4	33.8	66.2	21.9	79.4	1S,2S	1R,2S	0.82
3		Salen-Mn-SS	48	13.7	20.0	42.7	57.3	12.4	77.3	1S,2S	1R,2S	0.78
4		Salen-Mn-LS	72	13.8	27.5	48.6	51.4	13.3	77.9	1S,2S	1R,2S	0.89
5	*trans*-	Homo-[c]	6	100	100	100	n.d.	14.9	–	1R,2R	–	2.31
6		Salen-Mn-MCF	48	41.1	88.0	100	n.d.	14.0	–	1R,2R	–	1.68
7		Salen-Mn-SS	48	18.2	55.0	100	n.d.	11.0	–	1R,2R	–	1.41
8		Salen-Mn-LS	72	19.7	61.9	100	n.d.	11.4	–	1R,2R	–	1.20

Reaction temperature is 20 °C. The blank runs with the mixtures of *cis*/*trans*-methylstyrene, all support materials, dichloromethane, *n*-decane and 0.55 M NaClO exhibit that the physical adsorption of *cis*/*trans*-methylstyrene by SBA-15 is negligible.
[a] The molecular proportion of all epoxides in the products.
[b] The molecular proportion of *cis*- or *trans*-epoxide in the summary of all epoxides.
[c] Jacobsen catalyst from Acros.
[d] Facial turnover frequency (TOF) is calculated by the expression [product]/[catalyst] × time (s^{-1}) and according to the reaction data at 6 h. n.d., not detected.

metric epoxidation of 6-cyano-2,2-dimethylchromene catalyzed by an immobilized Jacobsen catalyst on different supports via the phenoxyl group [44], the ee value reached its maximum with an optimized pore size of 6.2 nm available in a SBA-15 support. A larger pore size of 7.6 nm led to lower ee values. DFT and QM/MM computational studies on the epoxidation reaction of *cis*/*trans*-β-methylstyrene catalyzed by anchored oxo-Mn^V-salen into MCM-41 channels suggested that the effect of the MCM-41 channel is steric rather than electronic and that the effect of channel confinement depends strongly on the channel size [39]. In the

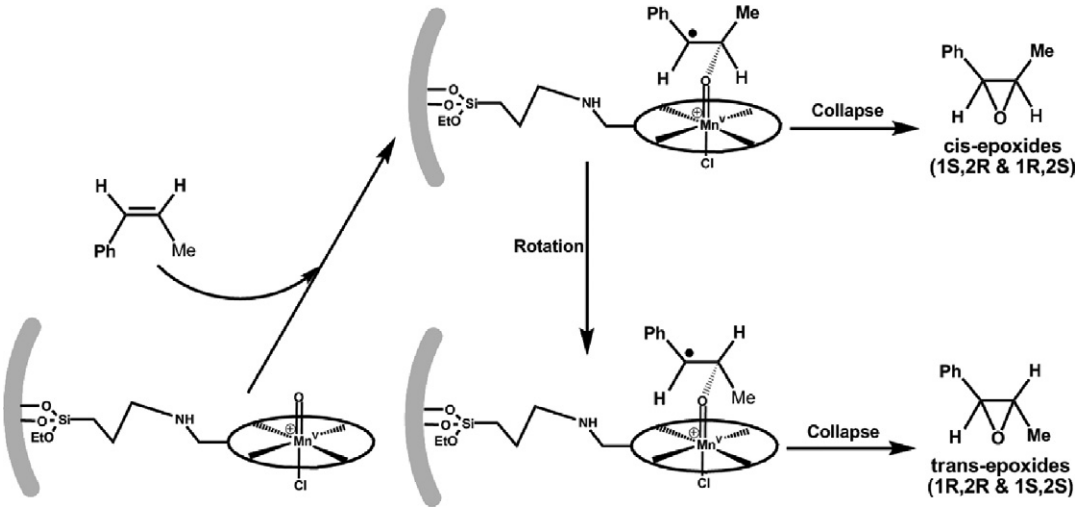

Scheme 4. Illustration of the mechanism for the asymmetric epoxidation of *cis*-β-methylstyrene catalyzed by immobilized Mn(salen) catalysts [13,36–42].

Table 4
Decomposition of β-methylstyrene epoxides catalyzed by Salen-Mn-LS

Epoxides	*t* (h)	Relative ratio for epoxides (1S,2R):(1S,2S):(1R,2R):(1R,2S)
cis-1S,2R	0	1:1.02:1.02:1.09
cis-1R,2S	24	1:1.03:1.03:1.06
trans-1S,2S	48	1:1.00:1.00:1.04
trans-1R,2R	72	1:1.01:0.99:1.05
	96	1:0.99:0.99:1.07

Reaction conditions are exactly as same as that for the asymmetric epoxidation tests.

present work, the ee values of *trans*-epoxides produced from *cis*-substrate in heterogeneous reactions decreased sequentially, but *trans*-1S, 2S epoxide was always the main product. The LS support had the smallest pore size, related to the lowest ee value for *trans*-epoxides. The more restricted environment of the nanochannels led to the lower enantioselectivity of the *trans*-epoxides produced from *cis*-substrate. However, in contrast to the varying ee values of the *trans*-epoxides, the restricted environment of the nanochannels in the heterogeneous systems exhibited no apparent effect on the enantioselectivity for *cis*-epoxides (entries 1, 2, 3, and 4, Tables 2 and 3). Our results suggest that the confinement effect of nanochannels on the collapse process is considerable for *trans*-intermediates but negligible for *cis*-intermediates.

Our findings also suggest possible increased production of *trans*-1R, 2R epoxide in the *trans*-route in nanochannels, which could explain the sequentially decreased ee values of *trans*-epoxides in heterogeneous reactions shown in Tables 2 and 3. In nanochannels, more *trans*-1R, 2R epoxide can be produced with a confinement effect on the ring-closure step of *trans*-intermediates, so that the ee values of *trans*-epoxides will decrease but with a configuration of *trans*-1S, 2S. Consistent with the tuning pore size of these three support materials, the ee value of *trans*-epoxides produced from *cis*-substrate in heterogeneous reactions was seen to decrease in the following sequence: homo-> MCF > SS > LS. A more homogeneous system-like environment, like that in MCF, benefits both the enantioselectivity of *trans*-epoxides and the production of *cis*-epoxides. For the epoxidation of *trans*-β-methylstyrene, only *trans*-epoxides were produced, and the heterogeneous and homogeneous reactions exhibited similar product distributions (Tables 2 and 3). This implies that in the epoxidaton of *cis*-β-methylstyrene, the rotation step from *cis*-intermediate to *trans*-intermediates is not reversible.

4. Conclusion

As demonstrated in Scheme 5, motion restriction and confinement effects in the nanochannels of support materials were found to affect the *cis*/*trans* ratio and enantioselectivity of *trans*-epoxides in heterogeneous asymmetric epoxidation of noncyclic olefins, such as *cis*-β-methylstyrene. The motion restriction in the nanochannels of immobilized Mn(salen) catalysts increased the likelihood of rotation for the sp^3 C–C single bond of *cis*-intermediate and resulted in more *trans*-epoxides in the heterogeneous reactions compared with the homogeneous reaction. Consistent with this increased *trans*-epoxide production, the enantioselectivity of *trans*-epoxides decreased in the heterogeneous reactions due to the significant confinement effect on the ring-closure step of the *trans*-intermediates. In contrast, the confinement effect of nanochannels on the collapse process of the *cis*-intermediates was negligible, and thus the ee values of the *cis*-epoxides hardly changed. Motion restriction and confinement effects can be tuned by changing the pore dimension and channel length of support materials, after which the production distribution of heterogeneous asymmetric epoxidation of *cis*-β-methylstyrene can be adjusted sequentially. Our findings also demonstrate that the rotation step from *cis*-intermediate to *trans*-intermediates is hardly reversible.

Acknowledgments

This work was supported by the Programme for Strategic Scientific Alliances (PSA) between China and the Netherlands (04-PSA-M-01, 2004CB720607, NSFC 20773123). The authors thank Pei Yuan, Chongqing University of Medical Sciences for his help with the FTIR tests; Dr. Xianliang Li from the Chongqing Entry-Exit Inspection and Quarantine Bureau for his help with the ICP-AES tests; Dr. Song Xiang, Hong Kong University for the helpful discussions; and Dr. Xin Zhan, University of Kentucky for his help with the English and overall manuscript preparation.

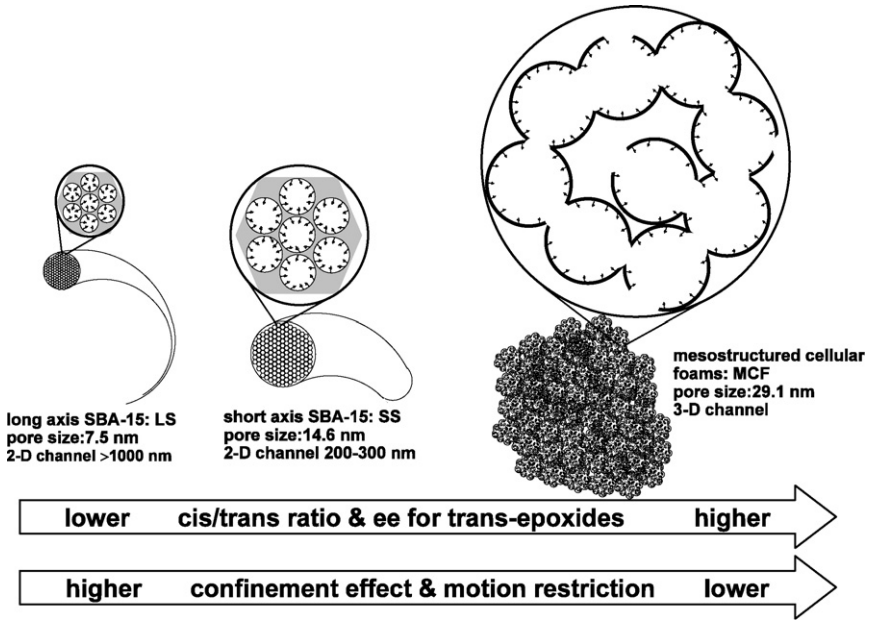

Scheme 5. Illustration of the confinement effect and motion restriction of nanochannels on heterogeneous asymmetric epoxidation.

References

[1] W. Zhang, J.L. Loebach, S.R. Wilson, E.N. Jacobsen, J. Am. Chem. Soc. 112 (1990) 2801.
[2] R. Irie, K. Noda, Y. Ito, N. Matsumoto, T. Katsuki, Tetrahedron Lett. 31 (1990) 7345.
[3] E.N. Jacobsen, W. Zhang, A.R. Muci, J.R. Ecker, L. Deng, J. Am. Chem. Soc. 113 (1991) 7063.
[4] C. Bianchini, P. Barbaro, Top. Catal. 19 (2002) 17.
[5] C.-E. Song, S.-G. Lee, Chem. Rev. 102 (2002) 3495.
[6] P. Mcmorn, G.J. Hutchings, Chem. Soc. Rev. 33 (2004) 108.
[7] C. Li, Catal. Rev. Sci. Eng. 46 (2004) 419.
[8] A. Corma, Catal. Rev. Sci. Eng. 46 (2004) 369.
[9] M. Heitbaum, F. Glorius, I. Escher, Angew. Chem. Int. Ed. 45 (2006) 4732.
[10] D.P. Serrano, J. Aguado, Appl. Catal. A 335 (2008) 172.
[11] S. Xiang, Y.L. Zhang, Q. Xin, C. Li, Chem. Commun. (2002) 2696.
[12] H.D. Zhang, S. Xiang, C. Li, Chem. Commun. (2005) 1209.
[13] H.D. Zhang, Y.M. Zhang, C. Li, J. Catal. 238 (2006) 369.
[14] T.S. Reger, K.D. Janda, J. Am. Chem. Soc. 122 (2000) 6929.
[15] D.W. Park, S.D. Choi, S.J. Choi, C.Y. Lee, G.J. Kim, Catal. Lett. 78 (2002) 145.
[16] V.D. Chaube, S. Shylesh, A.P. Singh, J. Mol. Catal. A Chem. 241 (2005) 79.
[17] M. Cardoso, A.R. Silva, B. de Castro, C. Freire, Appl. Catal. A 285 (2005) 110.
[18] I.K. Biernacka, A.R. Silva, A.P. Carvalho, J. Pires, C. Freire, Langmuir 21 (2005) 10825.
[19] R.I. Kureshy, I. Ahmad, N.H. Khan, S.H.R. Abdi, K. Pathak, R.V. Jasra, J. Catal. 238 (2006) 134.
[20] M. Holbach, M. Weck, J. Org. Chem. 71 (2006) 1825.
[21] B.M. Choudary, T. Ramani, H. Maheswaran, L. Prashant, K.V.S. Ranganath, K.V. Kumar, Adv. Synth. Catal. 348 (2006) 493.
[22] L.L. Lou, K. Yu, F. Ding, X.J. Peng, M.M. Dong, C. Zhang, S.X. Liu, J. Catal. 249 (2007) 102.
[23] F. Cozzi, Adv. Synth. Catal. 348 (2006) 1367.
[24] J.M. Thomas, R. Raja, D.W. Lewis, Angew. Chem. Int. Ed. 44 (2005) 6456.
[25] C. Li, H.D. Zhang, D.M. Jiang, Q.H. Yang, Chem. Commun. (2007) 547.
[26] M.E. Davis, Nature 417 (2002) 813.
[27] P. Piaggio, D. McMorn, P. Murphy, d. Bethell, P.C. Bullmanpage, F.E. Hancock, C. Sly, O.J. Kerton, G.J. Hutchings, J. Chem. Soc. Perkin Trans. 2 (2000) 2008.
[28] P.O. Norrby, J. Am. Chem. Soc. 117 (1995) 11035.
[29] D. Zhao, J. Feng, Q. Huo, N. Melosh, G.H. Fredrickson, B.F. Chmelka, G.D. Stucky, Science 279 (1998) 548.
[30] M. Choi, W. Heo, F. Kleitz, R. Ryoo, Chem. Commun. (2003) 1340.
[31] F. Minutolo, D. Pini, A. Petri, P. Salvadori, Tetrahedron Asymm. 7 (1996) 2293.
[32] D. Allen, E.N. Jacobsen, J. Am. Chem. Soc. 121 (1999) 4147.
[33] P. Fristrup, B.B. Dideriksen, D. Tanner, P.O. Norrby, J Am. Chem. Soc. 127 (2005) 13672.
[34] K.S.W. Sing, D.H. Everett, R.A.W. Haul, L. Moscou, R.A. Pierotti, J. Rouquerol, T. Siemieniewska, Pure Appl. Chem. 57 (1985) 603.
[35] W. Zhang, N.H. Lee, E.N. Jacobsen, J. Am. Chem. Soc. 116 (1994) 425.
[36] W. Zhang, E.N. Jacobsen, J. Org. Chem. 56 (1991) 2296.
[37] S. Chang, J. M Galvin, E.N. Jacobsen, J. Am. Chem. Soc. 116 (1994) 6937.
[38] W. Adam, K.J. Roschmann, C.R. Saha-Möller, D. Seebach, J. Am. Chem. Soc. 124 (2002) 5068.
[39] K. Malek, C. Li, R.A. Van Santen, J. Mol. Catal. A Chem. 271 (2007) 98.
[40] M. Palucki, P.J. Pospisil, W. Zhang, E.N. Jacobsen, J. Am. Chem. Soc. 116 (1994) 9333.
[41] S. Chang, N.H. Lee, E.N. Jacobsen, J. Org. Chem. 58 (1993) 6939.
[42] K. Malek, A.P.J. Jansen, C. Li, R.A. Van Santen, J. Catal. 246 (2007) 127.
[43] H.H. Lau, Angew. Chem. 73 (1961) 423.
[44] H.D. Zhang, C. Li, Tetrahedron 62 (2006) 6640.